Stabilization of a Native Protein Mediated by Ligand Binding Inhibits Amyloid Formation Independently of the Aggregation Pathway

Gemma Soldi, Georgia Plakoutsi, Niccolò Taddei, and Fabrizio Chiti*

Dipartimento di Scienze Biochimiche, Università di Firenze, Viale Morgagni 50, 50134 Firenze, Italy

Received June 1, 2006

The acylphosphatases from *Sulfolobus solfataricus* and *Drosophila melanogaster* (Sso AcP and AcPDro2) were previously shown to form amyloid-like aggregates without the need to unfold initially. Inorganic phosphate (P_i), a competitive inhibitor binding specifically to the active site of these proteins, was found to stabilize, upon binding, the native state of AcPDro2 and to inhibit its conversion into amyloid-like fibrils. The inhibitory effect of P_i is suppressed only in a variant in which the Arg residue responsible for P_i binding is mutated. The study on Sso AcP shows that P_i retards both the formation of the initial nativelike oligomers and their subsequent conversion into protofibrils. Thus, stabilization of the native structure mediated by specific binding with small molecules can be an effective therapeutic strategy against protein deposition diseases that originate from initially folded proteins, independently of the structure of the protein, its aggregation pathway, and the particular aggregated species responsible for pathogenesis.

1. Introduction

A number of pathological conditions are associated with the conversion of a specific protein or peptide from its soluble state into well organized fibrillar aggregates that accumulate in the extracellular space or inside the cells of fundamental tissues.[1−3] These disorders include neurodegenerative conditions, such as Alzheimer's, Parkinson's and Creutzfeldt−Jacob disease; nonneuropathic systemic amyloidoses, such as senile systemic amyloidosis, primary (light chain) systemic amyloidosis, and hemodialysis-related amyloidosis; and nonneuropathic localized diseases, such as type-II diabetes and pituitary prolactinoma.[1,3] The fibrillar assemblies, generally referred to as amyloid fibrils when they accumulate extracellularly, have the ability to bind specific dyes such as thioflavin T (ThT)[4,5] and Congo red (CR).[6,7] They consist of two to six protofilaments, each around 2−5 nm in diameter, that generally twist together to form fibrils that are typically 7−13 nm wide.[8] In each individual protofilament the protein molecules are arranged to form β-strands that run perpendicular to the long axis of the fibril.[9,10]

Some of the precursor proteins responsible for these pathological conditions are normally folded, in their soluble states, into globular units with persistent secondary structure and long-range interactions; examples include β2-microglobulin, transthyretin (TTR), lysozyme, immunoglobulin light chain, superoxide dismutase-type 1 (SOD-1), insulin, cystatin c, gelsolin, lactoferrin, and prolactin.[3,11] It is widely accepted, and supported by substantial evidence, that amyloid formation from an initially folded protein generally requires partial or total unfolding.[3,11−13] This "conformational change hypothesis" has led to the idea that small molecules binding specifically to the native tetramer of TTR could be effective therapeutic means against the various pathological conditions associated with amyloid deposition by TTR. Indeed, they were found to increase the free energy difference between the native tetramer of TTR and both the monomeric, partially folded state, and the tetramer dissociative transition state, therefore decreasing the equilibrium population of the amyloidogenic precursor(s) and/or increasing the kinetic barrier for TTR tetramer dissociation.[14,15] This idea has led to the search of hundreds of small molecules resembling the chemical structure of thyroxine and having therefore an ability to bind to the native tetramer of the protein by occupying the two natural binding sites at the dimer−dimer interfaces.[16]

Along the same lines it was found that ligands binding to the native state of human muscle acylphosphatase inhibits fibril formation with an efficacy that correlates with ligand concentration and binding constant.[17] In another study, a cavity at the monomer−monomer interface of native SOD-1 was exploited to identify, by an in silico screening approach, a number of compounds binding to the native dimer of SOD-1 and inhibiting aggregation.[18] Finally, a single-domain fragment of a camelid antibody binding to native human lysozyme was also found to inhibit aggregation.[19]

Although the conformational change hypothesis is certainly appropriate to explain the aggregation behavior of many folded proteins, evidence is mounting that proteins retain a small yet significant propensity to aggregate when folded into their native structures. Models in which partial or complete unfolding is ruled out, at least in the initial step(s) of the complex process of fibril formation, have been described for human insulin,[20] Ure2p from *Saccharomyces cerevisiae*,[21] the variable domain of an immunoglobulin light chain (called LEN),[22] human lithostathine,[23] the acylphosphatase from *Sulfolobus solfataricus*,[24,25] the S6 protein from *Thermus* thermophilus,[26] human ataxin-3[27] and the isoform 2 of acylphosphatase from *Drosophila melanogaster*.[28]

If a globular protein undergoes aggregation without unfolding, at least in the early steps of the process of self-assembly when the first oligomers form, the question naturally arises as to whether strategies designed to stabilize the globular native state represent an effective therapeutic means to inhibit aggregation and contrast disease onset. This is an important issue as it is increasingly recognized that the small oligomers, rather than the mature fibrils, represent the pathogenic species in many protein deposition diseases. In this work we use the acylphosphatases from *D. melanogaster* (AcPDro2) and *S. solfataricus* (Sso AcP) to explore the effect on amyloid aggregation of a ligand binding specifically to the native states of these two proteins. Unlike other acylphosphatases so far investigated,

* Corresponding author. Tel.: +390554598319. Fax: +390554598905. E-mail: fabrizio.chiti@unifi.it.

10.1021/jm0606488 CCC: $33.50 © 2006 American Chemical Society
Published on Web 09/02/2006

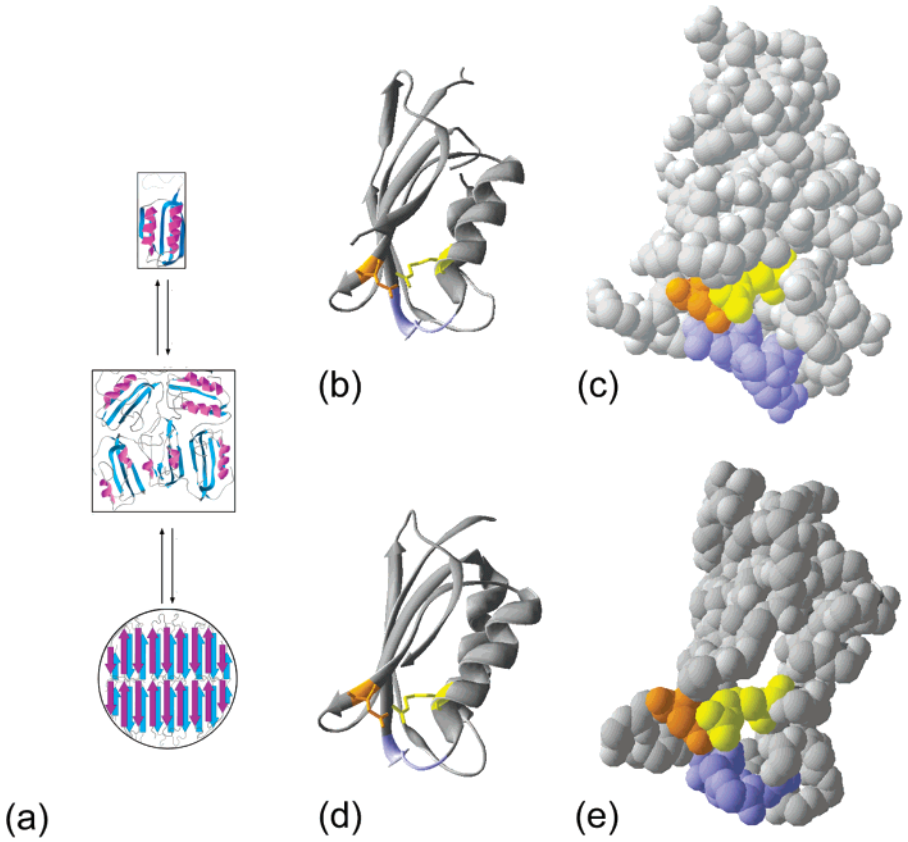

Figure 1. Three-dimensional structures and aggregation pathways of AcPDro2 and Sso AcP. (a) Mechanisms of aggregation of AcPDro2 into amyloid-like fibrils or Sso AcP into amyloid protofibrils, under conditions in which both proteins are initially native. Both proteins were shown to undergo assembly and, subsequently, a structural reorganization to form amyloid-like structures. Reprinted with permission from *Journal of Molecular Biology* (Plakoutsi, G.; Bemporad, F.; Calamai, M.; Taddei, N.; Dobson, C. M.; Chiti, F. Evidence for a mechanism of amyloid formation involving molecular reorganisation within native-like precursor aggregates. *J. Mol. Biol.* **2005**, *351*, 910−922[25]). Copyright 2005, with permission from Elsevier. (b,c,d,e) Three-dimensional structures of native AcPDro2 (b,c) and Sso AcP (d,e) shown by secondary structure (b,d) and space-fill (c,e) representation as determined by X-ray crystallography (PDB codes are 1URR and 2BJD, respectively).[31,32] In all structures, residues of the active site are shown in yellow (Arg27 and Arg30 in AcPDro2 and Sso AcP, respectively), orange (Asn45 and Asn48, respectively), and blue (residues GXVQGV at positions 19−24 and 22−27, respectively). All structures are obtained using the SwissPDBViewer software.

namely the N-terminal domain of *Escherichia coli* HypF (HypF-N) and human muscle acylphosphatase,[29,30] AcPDro2 and Sso AcP were previously shown to aggregate, under conditions in which their native states are initially populated, by forming assemblies in which the proteins retain a nativelike structure that only later converts into amyloid-like protofibrils and/or fibrils (Figure 1a).[24,25,28]

Similarly to all the acylphosphatases so far characterized, AcPDro2 and Sso AcP are α/β proteins with a ferredoxin-like fold in their native states (Figure 1b,d)[31,32] and an ability to catalyze the hydrolysis of acyl phosphates.[32,33] From structural inspection and a detailed mutational study carried out on the homologous human muscle acylphosphatase,[34−36] the active site of AcPDro2 appears to be formed by Arg27, Asn45, and the loop 19−24 (Figure 1b,c). These correspond to Arg30, Asn48, and loop 22−27 for Sso AcP (Figure 1d,e). The Arg residue is mainly involved in acyl phosphate binding, whereas the Asn residue binds to the water molecule, promoting hydrolysis, and participates in catalysis.[34,35] Importantly, the active site can also bind specifically, by means of the Arg residue, to a number of competitive inhibitors containing either a phosphate or sulfate group.[17,37] P_i (inorganic phosphate) was confirmed to be a competitive inhibitor for both AcPDro2 and Sso AcP, thus with an ability to bind to the active site of these two proteins in their native states.[32,33]

The kinetically well characterized pathways of amyloid aggregation for AcPDro2 and Sso AcP and the ability of their native states to bind specifically to an ion as simple as P_i make these two proteins ideal systems to investigate whether compounds binding specifically to the native folded states of amyloidogenic proteins can be effective drugs even for cases in which unfolding may not be the primary step in amyloidogenesis.

2. Results

2.1. P_i Stabilizes Native AcPDro2 and Inhibits Its Conversion into Amyloid-like Fibrils. AcPDro2 was previously shown to form, in 5% (v/v) trifluoroethanol (TFE) at pH 5.5 and 25 °C, aggregates with a morphology and diameter typical of amyloid fibrils, a high content of β-sheet structure, and an ability to bind CR and ThT.[28] Under such conditions AcPDro2 was found to have, before aggregation, a fully native structure; moreover, it was also shown to have a conformational stability, expressed as free energy change of unfolding ($\Delta G_{U-F}^{H_2O}$), apparently identical to that determined in the absence of TFE, i.e., under conditions in which the protein does not aggregate.[28] The time-course of fibril formation was shown to be remarkably more rapid than that expected from models in which the protein is viewed to unfold before assembly, leading to the aggregation scheme reported in Figure 1a.[28]

We first investigated whether P_i, a competitive inhibitor binding to the active site of all acylphosphatases so far investigated including AcPDro2,[33] stabilizes the native structure of AcPDro2 relative to the fully unfolded state. Figure 2a shows

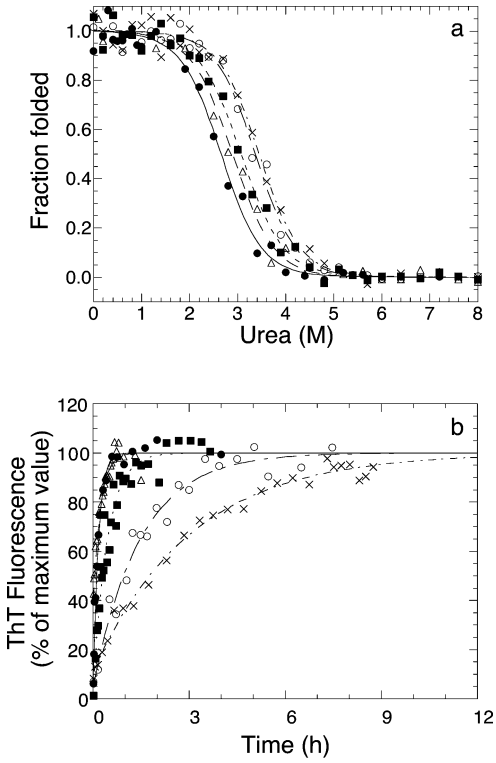

Figure 2. (a) Equilibrium urea unfolding curves of wild-type AcPDro2 in 0 mM (●), 1 mM (△), 2 mM (■), 5 mM (○), and 10 mM (×) P_i. The lines represent the best fits to the two-state equation previously described.[38] (b) Time-course of aggregation of 0.4 mg mL^{-1} wild-type AcPDro2 in 10% (v/v) TFE with various amounts of P_i (symbols as in Figure 2a). The zero time point refers to the addition of TFE to the protein solution. The lines through the data represent the best fits to a single-exponential function (eq 1). In both panels conditions were 50 mM acetate, 2 mM DTT, pH 5.5, 25 °C.

Table 1. Parameters for Enzymatic Activity, Equilibrium Unfolding, and Aggregation of AcPDro2 Variants

variant	specific activity (IU mg^{-1})[a]	C_m (M)[b]	$\Delta G_{U-F}^{H_2O}$ (kJ mol^{-1})[b,c]	k_{obs} (s^{-1})[d]
wt/0 mM P_i	1280	2.65 ± 0.1	15.5 ± 0.7	1.7(±0.1)·10^{-3}
wt/1 mM P_i		2.9 ± 0.1	16.9 ± 0.7	1.2(±0.1)·10^{-3}
wt/2 mM P_i		3.1 ± 0.1	17.9 ± 0.7	6.3(±0.6)·10^{-4}
wt/5 mM P_i		3.35 ± 0.1	19.6 ± 0.7	1.9(±0.2)·10^{-4}
wt/10 mM P_i		3.45 ± 0.1	20.1 ± 0.7	9.1(±0.6)·10^{-5}
R27A/0 mM P_i	not detectable (~0)	4.3 ± 0.1	25.1 ± 0.8	3.5(±0.5)·10^{-3}
R27A/5 mM P_i		4.45 ± 0.1	25.9 ± 0.8	4.0(±0.5)·10^{-3}
N45A/0 mM P_I	not detectable (~0)	3.3 ± 0.1	19.4 ± 0.7	6.1(±0.3)·10^{-4}
N45A/5 mM P_i		3.7 ± 0.1	21.6 ± 0.7	2.3(±0.2)·10^{-4}

[a] Determined in 50 mM acetate buffer, pH 5.5, 25 °C, using 4 mM benzoyl phosphate as a substrate. IU = international units. [b] Determined from equilibrium urea-unfolding experiments analyzed according to a two-state model (Santoro and Bolen[38]). [c] $\Delta G_{U-F}^{H_2O}$ values were calculated using $\Delta G_{U-F}^{H_2O} = \langle m \rangle C_m$, where $\langle m \rangle$ equals 5.8 ± 0.1 kJ mol^{-1} M^{-1} (the average m value from all the acquired curves). [d] Aggregation rate constants determined from time courses of ThT fluorescence analyzed with eq 1. Conditions were 10%, 13%, and 11% (v/v) TFE for wild-type, R27A, and N45A AcPDro2, respectively.

urea-induced unfolding curves acquired at equilibrium in the presence of increasing concentrations of P_i and obtained using intrinsic fluorescence as a spectroscopic probe to follow unfolding. The analysis of the curves, carried out using a two-state model,[38] yielded for each of the investigated P_i concentrations, the values of unfolding midpoint (C_m), cooperativity (m value), and free energy of unfolding extrapolated in the absence of denaturant ($\Delta G_{U-F}^{H_2O}$). These are reported in Table 1. The C_m value appears to increase with P_i concentration (Figure 2a and Table 1). Since the m value appears to be substantially similar under the various conditions, the $\Delta G_{U-F}^{H_2O}$ also appears to increase with P_i concentration (Table 1).

We then studied amyloid fibril formation of AcPDro2 at P_i concentrations ranging from 0 to 10 mM. Under such conditions AcPDro2 is initially native (data not shown). Fibril formation of AcPDro2, followed using the ThT fluorescence assay, was found to be increasingly slower as the P_i concentration increases (Figure 2b and Table 1).

2.2. P_i Has No Effect on an AcPDro2 Mutant Lacking the Main Residue Involved in Binding. To investigate further whether the inhibitory effect of P_i on amyloid formation arises from the ability of this compound to bind to and stabilize the protein in its native conformation or rather from another nonspecific effect, two single mutants of AcPDro2 were produced, having Arg27 and Asn45 substituted with alanine, respectively (R27A and N45A AcPDro2). From a detailed study carried out on the homologous human muscle acylphosphatase,[34] Arg27 is known to be the main binding site of both the substrate and competitive inhibitor. Accordingly, R27A AcPDro2 appears to be enzymatically inactive (Table 1) and does not appear to be stabilized by the addition of 5 mM P_i (Figure 3a, Table 1). In addition to having no stabilizing effect of the native structure of AcPDro2, P_i was also found to have no detectable effect on the fibril formation rate of AcPDro2, at the same concentration of 5 mM (Figure 3b). This allows the P_i-mediated inhibition of amyloid fibril formation to be closely linked to the ability of the compound to bind to, and stabilize, the native structure of the protein.

2.3. P_i Inhibits Amyloid Formation of a Catalytically Inactive Variant in Which P_i Binding Is Retained. Asn45 is thought to be mainly involved in catalysis, rather than substrate and P_i binding, from the study performed on the corresponding Asn41 of human muscle acylphosphatase.[35] N45A AcPDro2 has lost its acylphosphatase activity (Table 1) but can still bind to, and be stabilized by, P_i (Table 1 and Figure 3c). The increases of C_m and $\Delta G_{U-F}^{H_2O}$ following the addition of 5 mM P_i were 0.40 M and 2.2 kJ mol^{-1}, respectively (Table 1). These values were lower than those of the wild-type protein (0.7 M and 4.1 kJ mol^{-1}, respectively), indicating that although the N45A mutant retains an ability to bind to P_i, it does so with a lower binding affinity. Fibril formation of N45A AcPDro2 is significantly retarded in the presence of 5 mM P_i (Figure 3d), although the deceleration is only 2.6-fold and lower than that of the wild-type protein, 8.9-fold (Table 1). This result can be effectively explained by considering that the native state of the N45A mutant has a retained, but decreased, ability to bind to P_i relative to the wild-type protein.

2.4. P_i Slows Down the Formation of Nativelike Oligomers by Sso AcP. Sso AcP is a hyperthermophilic protein with a $\Delta G_{U-F}^{H_2O}$ of 48 kJ mol^{-1} at pH 5.5, 37 °C,[39] with unfolding occurring only under very harsh conditions.[32] In 15−25% (v/v) TFE, pH 5.5, 25 °C, the protein populates, before aggregation initiates, a nativelike conformation.[24] On the time scale of 1−2 min, oligomers form in which the protein molecules retain a marked enzymatic activity.[25] These species do not yet bind CR, ThT, and 1-anilino-8-naphthalenesulfonic acid (ANS) nor do they show an extensive β-sheet structure, as revealed by far-ultraviolet circular dichroism (far-UV CD) and Fourier transform infrared spectroscopy (FTIR).[25] Despite a nativelike topology, the secondary structure appears to be changed to some extent.[25]

These oligomers further convert directly, on the time scale of several minutes with no need of dissociation and renucleation, into another type of aggregate which binds CR, ThT, and ANS;

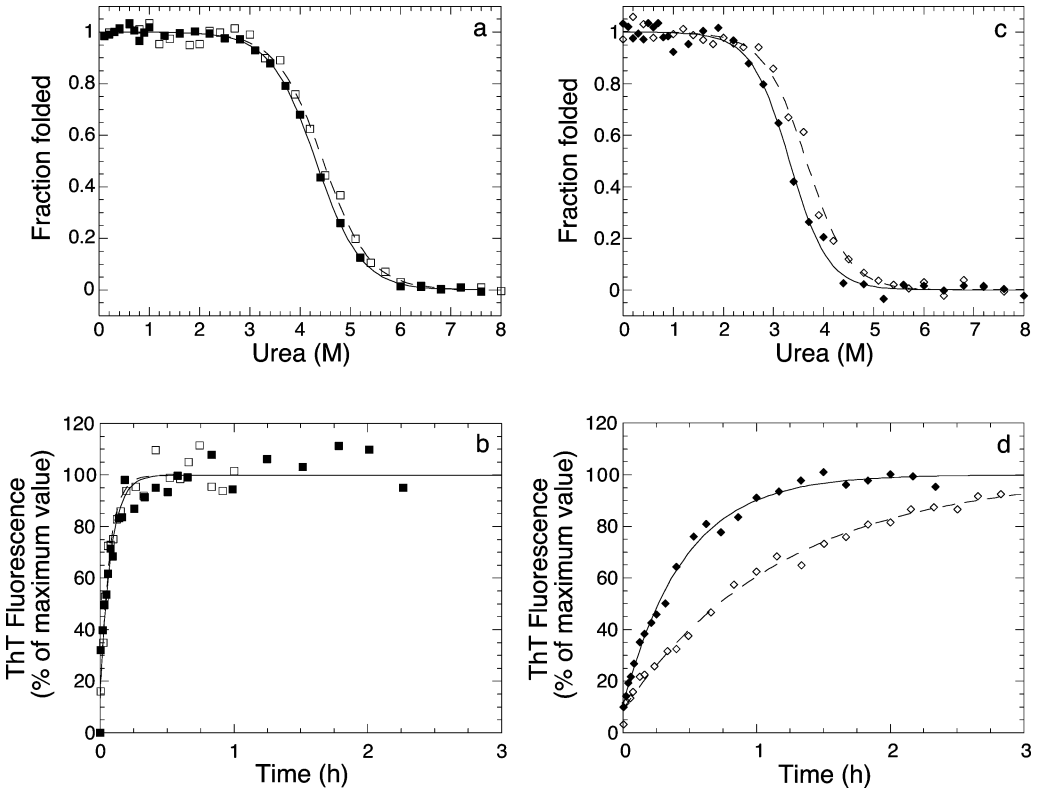

Figure 3. (a,c) Equilibrium urea unfolding curves for R27A (a) in 0 mM (■) and 5 mM (□) P_i, and for N45A (c) in 0 mM (◆) and 5 mM (◇) P_i. The lines represent the best fits to the two-state equation previously described.[38] (b,d) Time-course of aggregation of 0.4 mg mL^{-1} R27A (b) and N45A (d) in solutions containing 0 mM and 5 mM P_i (symbols as in panels a and c). For both b and d, the zero time point refers to the addition of TFE to the protein solution. The lines through the data represent the best fits to a single-exponential function (eq 1). Experimental conditions were 0% (a,c), 13% (b), or 11% (d) TFE, 50 mM acetate buffer, 2 mM DTT, pH 5.5, 25 °C.

possesses extensive β-sheet structure; and lacks enzymatic activity.[25] Using transmission electron microscopy these species appear to have a morphology typical of amyloid protofibrils, i.e., spherical aggregates with a diameter of 3−5 nm, or chainlike aggregates in which the constituent beads again have a diameter of 3−5 nm.[25] Formation of the first and second types of aggregates occurs 2 and 4 orders of magnitude more rapidly than unfolding of the native monomer under the same conditions, ruling out the need to unfold to initiate aggregation (Figure 1a).[24] Our ability to resolve on the time scale the formation of the nativelike oligomers and their further conversion into amyloid protofibrils provides a unique opportunity to investigate the effect of P_i on the two aggregation phases separately.

Self-assembly of native monomers into nativelike oligomers can be effectively followed by monitoring the change of either light scattering intensity or ellipticity at 208 nm ($[\theta]_{208}$), since the difference of the CD signals is maximal at this wavelength.[40] The apparent rate constants obtained with the two experimental spectroscopic probes are essentially similar.[40] We have therefore chosen to use far-UV CD for analyzing the effect of P_i on this oligomerization step. Incubation of wild-type Sso AcP in 20% (v/v) TFE yields a rapid increase of $[\theta]_{208}$ followed by a much slower increase (Figure 4a), with these changes attributable to the first and second aggregation phases, respectively.[40] The addition of 1 or 2 mM P_i causes the first rapid increase of $[\theta]_{208}$ to be slower and lower in magnitude (Figure 4a,b). This indicates that P_i slows down the formation of the native oligomers and causes the conformational change associated with their formation to be less significant than in the absence of P_i. The CD traces obtained for wild-type Sso AcP in the presence of P_i are characterized by small but significant exponential changes of CD signal, although these are visually masked by the relatively high signal-to-noise ratio (Figure 4a). The traces could therefore be analyzed with a procedure of best fit using eq 2 (Figure 4a, solid line) to yield the rate constants reported in Figure 4b.

P_i has no effect and a significant decelerating effect on this aggregation phase for the R30A and N48A mutants of Sso AcP, respectively (corresponding to the R27A and N45A variants for AcPDro2). In the presence of P_i, R30A Sso AcP assembles with a rate even higher than that of the wild-type protein in the absence of P_i (Figure 4a), probably as a result of the effect of the mutation on aggregation (the mutation decreases the net charge of Sso AcP, thus facilitating aggregation relative to the wild-type). By contrast, aggregation of the N48A mutant in the presence of 1 mM P_i appears to be slower, and involve a lower amplitude change of $[\theta]_{208}$, than for the wild-type protein in the absence of the ligand (Figure 4a). These results allow the inhibitory effect of P_i on the formation of nativelike oligomers to be coupled again to the specific binding of the ligand with the native monomeric protein.

2.5. P_i also Decelerates the Conversion of Nativelike Oligomers into Amyloid-like Protofibrils. The second step of aggregation, that is the conversion of the nativelike oligomers into the amyloid-like protofibrils, can be followed by monitoring the exponential increase of ThT fluorescence as previously reported.[25,40] Such an exponential increase is protein concentration independent, as it involves a structural conversion within a preformed aggregate rather than being rate-limited by the assembly of two or more protein molecules.[25] This aggregation step appears to be decelerated markedly by 1 mM P_i for wild-type Sso AcP (Figure 5). This suggests that P_i can still bind to, and stabilize, the nativelike aggregates (which indeed are enzymatically active and possess the ability to bind the substrate) and disfavors their conversion into amyloid protofibrils in which

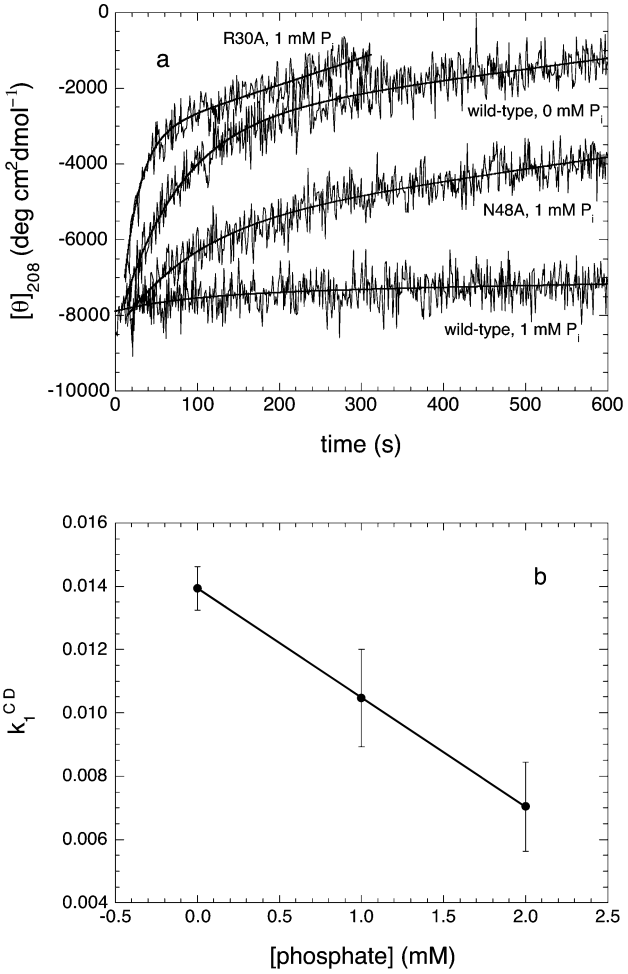

Figure 4. (a) Self-assembly of native, monomeric Sso AcP into nativelike oligomers followed by far-UV CD at 208 nm. The four traces refer to wild-type Sso AcP with and without P_i, R30A Sso AcP with P_i, and N48A Sso AcP with P_i, as indicated in the graph. The solid lines through the traces represent the best fits to eq 2. The resulting rate constant is called k_1^{CD}. Experimental conditions were 20% (v/v) TFE, 50 mM acetate, pH 5.5, 25 °C. (b) Dependence of k_1^{CD}, obtained for wild-type Sso AcP, on P_i concentration. Experimental conditions were as in panel a.

the nativelike topology, enzymatic activity, and binding properties are lost. The same aggregation step for the R30A variant in the presence of 1 mM P_i was found to occur with a rate apparently identical to that found for the wild-type protein in the absence of P_i (Figure 5), lending further support to the importance of binding specificity. Accordingly, the nativelike aggregates of N45A Sso AcP, in which the substituted residue is involved in catalysis but not substrate binding, convert more slowly in the presence of P_i relative to the wild-type protein in its absence (Figure 5).

3. Discussion

Several works have demonstrated that that the binding of a ligand to the native state of a folded protein is an effective therapeutic strategy to inhibit amyloid formation, when this process requires at least partial unfolding or disruption of the native quaternary structure.[14,16−19] The results presented here suggest that the ligand-mediated stabilization of the native state is also an effective strategy to inhibit amyloid formation even when the process does not require unfolding as an early step to trigger the process of assembly. Both of the globular proteins used here aggregate more slowly in the presence of a ligand

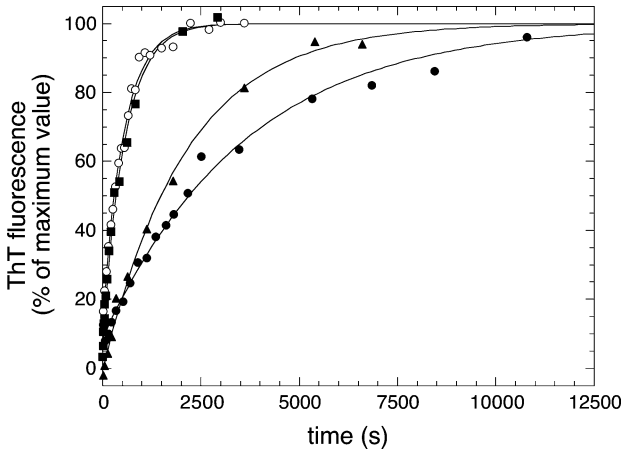

Figure 5. Conversion of nativelike oligomers of Sso AcP into amyloid protofibrils followed by ThT fluorescence. The traces refer to wild-type Sso AcP without (○) and with (●) 1 mM P_i, R30A Sso AcP with 1 mM P_i (■), and N45A Sso AcP with 1 mM P_i (▲). The solid lines through the data points represent the best fits to exponential functions (eq 1). Experimental conditions were as in Figure 4a.

that acts physiologically as a competitive inhibitor and hence binds specifically to the active site of the native state. In both proteins the inhibitory effect is no longer present when the main substrate and inhibitor-binding residue is substituted (Arg27 and Arg30 for AcPDro2 and Sso AcP, respectively), whereas it is maintained when the main catalytic site that is not involved in binding is replaced (Asn45 and Asn48 for AcPDro2 and Sso AcP, respectively). Although the two proteins used here are not involved in any protein deposition disease and P_i binds to them with an affinity that could not be exploitable in pharmacological research, these results underlie the concept that stabilization of the native conformation of amyloidogenic proteins by specific binding can represent a strategy of general interest for inhibiting aggregation and amyloid formation in vivo.

In the aggregation process of Sso AcP, where the formation of the nativelike oligomers can be studied independently of their later conversion into amyloid-like protofibrils, the ligand appears to retard both aggregation phases. These findings indicate that following binding with the ligand both the monomeric native state and the early oligomeric nativelike species are stabilized, whereas the transition state for their interconversion is affected to a lower extent or is not affected at all (Figure 6). Similarly, the transition state for the conversion of the initial oligomers into the protofibrils is stabilized only marginally relative to the nativelike oligomers. The amyloid protofibrils, in which the individual protein molecules have undergone a major conformational change, have presumably lost completely their affinity for the ligand and therefore are not stabilized upon ligand addition. In this scenario, the free energy barriers for both aggregation phases increase in the presence of ligand, explaining the deceleration of both aggregation phases following the addition of P_i.

These results are in agreement with previously reported findings showing that destabilized mutants of Sso AcP form the early nativelike oligomers and undergo the further conversion into amyloid protofibrils more rapidly than the wild-type protein.[40] Although in the initial oligomers the individual protein molecules have maintained a nativelike topology and enzymatic activity, far-UV CD and FTIR indicate that the protein has undergone a small but significant structural change after the transition.[25] Such an aggregation event is therefore promoted by structural fluctuations, but not unfolding, that are facilitated by destabilizing mutations, but are certainly disfavored by the

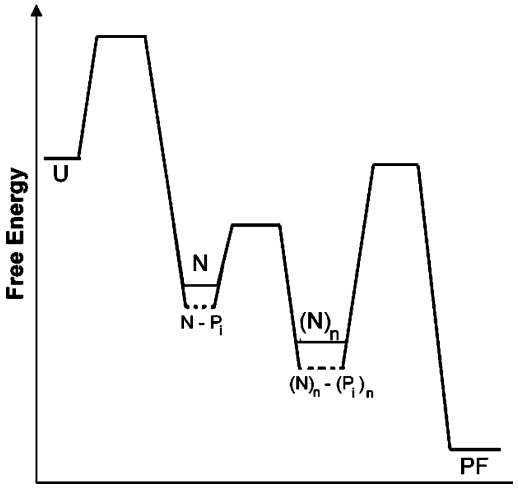

Figure 6. The effect of P_i on the aggregation process of Sso AcP. P_i binds to the monomeric native conformation N and the early oligomers in which the protein molecules retain a nativelike conformation, $(N)_n$. Their absolute free energies decrease upon binding (dashed lines). The unfolded state U and the amyloid-like protofibrils PF do not bind to P_i and their free energies remain unaffected in the presence of the ligand. P_i may also bind to one or all the transition states reported in the scheme, but with lower affinity, as their energies are found to decrease to a small extent, if at all. As a result of these effects, P_i slows down the formation of both $(N)_n$ and PF.

"freezing" of the native structure in the protein−ligand complex. The rate of the second phase of aggregation also increases with destabilzing mutations and decreases following the addition of the ligand. In this case a substantial and global structural conversion has to occur from the nativelike molecules into an amyloid protofibrillar state in which there is apparently no detectable sign of nativelike structural elements.

4. Conclusions

Addition of a ligand binding specifically to the native structure of a protein inhibits aggregation into amyloid structures when partial unfolding or disruption of the quaternary structure is required to initiate aggregation.[14,16,18,19] Here we have shown that ligands also inhibit amyloid formation when the process does not require unfolding as an initial step but assembly into nativelike structures that later convert into amyloid structures. This indicates that the structure-based design of ligands binding with high affinity to the native soluble state of an amyloidogenic protein, either to the active site, allosteric site, or any other cavity that may act as a binding pocket as elegantly shown,[18] can be a valid, generic therapeutic strategy to inhibit amyloid formation in pathological states, at least for those associated with proteins adopting globular folded conformations in their native states. This therapeutic approach can be effective not just because it is independent of the aggregation pathway but also because it interferes with the thermodynamics and kinetics of the very early steps of the aggregation process, therefore resulting in the inhibition of any early oligomeric species, including nativelike oligomers, that are increasingly thought to be pathogenic species in many protein deposition diseases.

5. Materials and Methods

5.1. Materials, Protein Purification, and Site-Directed Mutagenesis. ThT, TFE, dithiothreitol (DTT), and urea were purchased from Sigma-Aldrich. Benzoyl phosphate was synthesized and purified as described.[41] The genes of AcPDro2 and Sso AcP were cloned in pGEX-4T1 and pGEX-2T plasmids, respectively (Amersham Biosciences, Uppsala, Sweden), and expressed in DH5α *E. coli* cells as proteins fused to glutathione-S-transferase (GST). The resulting proteins were purified and separated from GST according to the plasmid manufacturer. AcPDro2 was stored in 50 mM acetate buffer, 2 mM DTT, pH 5.5. Sso AcP was stored in 10 mM Tris-HCl, pH 8.0. Protein concentration was determined spectrophotometrically using ϵ_{280} values of 1.09 and 1.24 mL mg^{-1} cm^{-1} for AcPDro2 and Sso AcP, respectively. Before starting each experiment, each protein solution was centrifuged at 18 000 rpm for 3−5 min and filtered using 0.02 μm Anotop 10 filters (Whatman International Ltd, Maidstone, UK). The mutated genes of AcPDro2 and Sso AcP were created using the QuickChange site-directed mutagenesis kit from Stratagene (La Jolla, CA). The presence of the desired mutation was assessed by sequencing the entire gene. All mutational variants were expressed in *E. coli* XL-1 Blue cells and purified similarly to the corresponding wild-type proteins.

5.2. Enzymatic Activity. Enzymatic activity was tested using a final protein concentration of 0.5 μg mL^{-1} and 4 mM benzoyl phosphate as a substrate, as described.[42] Other experimental conditions were 50 mM acetate buffer, 2 mM DTT, pH 5.5, 25 °C. A Perkin-Elmer λ 4 B UV−vis spectrophotometer was used (Wellesley, MA). The noncatalyzed spontaneous hydrolysis of benzoyl phosphate was subtracted from all measurements.

5.3. ThT Assay. AcPDro2 and Sso AcP were incubated at concentrations of 0.4 mg mL^{-1} in 50 mM acetate buffer, 2 mM DTT, pH 5.5, 25 °C, containing P_i at a concentration ranging from 0 to 10 mM and TFE [10 and 20% (v/v) TFE for AcPDro2 and Sso AcP, respectively]. At regular times 60-μL aliquots of each sample were added to 440 μL of a solution containing 25 μM ThT, 25 mM phosphate buffer, pH 6.0, immediately before collecting the ThT fluorescence value. The steady-state fluorescence values of the resulting samples were measured at 25 °C using a 2 × 10 mm path length quartz cuvette and a Perkin-Elmer LS 55 spectrofluorimeter (Wellesley, MA) equipped with a thermostated cell holder attached to a Haake F8 water bath (Karlsruhe, Germany). The excitation and emission wavelengths were 440 and 485 nm, respectively.[4] All measured fluorescence values are given after subtracting the fluorescence measured in the absence of protein and normalized so that the final fluorescence at the endpoint of the kinetic trace was 100%. ThT fluorescence was plotted versus time and fitted to

$$F(t) = F_{eq} + A \exp(-k_{obs}t) \quad (1)$$

where $F(t)$ is the ThT fluorescence at time t, F_{eq} is the maximum ThT fluorescence obtained at the end of the observed exponential phase, A is the amplitude of the fluorescence change, and k_{obs} is the apparent rate constant.

5.4. Far-UV Circular Dichroism. The aggregation process of Sso AcP was started by incubating the protein, at a concentration of 0.4 mg mL^{-1}, in 20% (v/v) TFE, 50 mM acetate buffer, pH 5.5, 25 °C, in the presence of 0−10 mM P_i. The ellipticity at 208 nm was followed at 25 °C using a 1 mm path length quartz cuvette and a Jasco J-810 spectropolarimeter (Tokyo, Japan) equipped with a thermostated cell holder attached to a Thermo Haake C25P water bath (Karlsruhe, Germany). For each kinetic trace, the ellipticity values were blank-subtracted, normalized to the mean residue ellipticity ($[\theta]_{208}$), plotted versus time, and fitted to

$$[\theta]_{208}(t) = [\theta]_{208}(\mathrm{eq}) + A \exp(-k_{obs}t) + a + bt \quad (2)$$

where $[\theta]_{208}(t)$ is the mean residue ellipticity at 208 nm at time t, $[\theta]_{208}(\mathrm{eq})$ is the value obtained at the end of the observed exponential phase, A is the amplitude of the $[\theta]_{208}$ change, k_{obs} is the apparent rate constant, a and b are the coefficients of the slower kinetic phase that on this relatively short time scale can be approximated to a straight line.

5.5. Equilibrium Unfolding. Unfolding of AcPDro2 was studied at equilibrium in the presence of different concentrations of P_i, ranging from 0 to 10 mM. For each P_i concentration, 25−30 samples were prepared containing 0.02 mg mL^{-1} protein in 50 mM acetate buffer, 2 mM DTT, pH 5.5, and various urea concentrations

ranging from 0.1 to 8 M. The samples were left to equilibrate for a few minutes at 25 °C. Far-UV CD spectra were acquired at 25 °C using the apparatus described in the previous paragraph and processed using the adaptive smoothing method.[43] The ellipticity at 222 nm was plotted versus urea concentration and the resulting plot was fitted to the equation previoulsy described.[38]

Acknowledgment. This work was supported by grants from the European Union (Project HPRN-CT-2002-00241), the Italian MIUR (FIRB project no. RBNE03PX83; PRIN project no. 2005027330), and the EMBO Young Investigator Programme (EMBO YIP 2005).

References

(1) Selkoe, D. J. Folding proteins in fatal ways. *Nature* **2003**, *426*, 900−904. Erratum. *Nature* **2004**, *428*, 445.
(2) Merlini, G.; Bellotti, V. Molecular mechanisms of amyloidosis. *N. Engl. J. Med.* **2003**, *349*, 583−596.
(3) Chiti, F.; Dobson, C. M. Protein misfolding, functional amyloid and human disease. *Annu. Rev. Biochem.* **2006**, *75*, 333−366.
(4) LeVine, H., 3rd. Quantification of beta-sheet amyloid fibril structures with thioflavin T. *Methods Enzymol.* **1999**, *309*, 274−284.
(5) Krebs, M. R.; Bromley, E. H.; Donald, A. M. The binding of thioflavin-T to amyloid fibrils: Localisation and implications. *J. Struct. Biol.* **2005**, *149*, 30−37.
(6) Klunk, W. E.; Jacob, R. F.; Mason, R. P. Quantifying amyloid by Congo red spectral shift assay. *Methods Enzymol.* **1999**, *309*, 285−305.
(7) Jin, L. W.; Claborn, K. A.; Kurimoto, M.; Geday, M. A.; Maezawa, I.; Sohraby, F.; Estrada, M.; Kaminksy, W.; Kahr, B. Imaging linear birefringence and dichroism in cerebral amyloid pathologies. *Proc. Natl. Acad. Sci. U.S.A.* **2003**, *100*, 15294−15298.
(8) Serpell, L. C.; Sunde, M.; Benson, M. D.; Tennent, G. A.; Pepys M. B.; Fraser, P. E. The protofilament substructure of amyloid fibrils. *J. Mol. Biol.* **2000**, *300*, 1033−1039.
(9) Sunde, M.; Blake, C. The structure of amyloid fibrils by electron microscopy and X-ray diffraction. *Adv. Protein Chem.* **1997**, *50*, 123−159.
(10) Tycko, R. Insights into the amyloid folding problem from solid-state NMR. *Biochemistry* **2003**, *42*, 3151−3159.
(11) Uversky, V. N.; Fink, A. L. Conformational constraints for amyloid fibrillation: The importance of being unfolded. *Bioch. Biophys. Acta* **2004**, *1698*, 131−153.
(12) Kelly, J. W. The alternative conformations of amyloidogenic proteins and their multi-step assembly pathways. *Curr. Opin. Struct. Biol.* **1998**, *8*, 101−106.
(13) Dobson, C. M. Protein folding and misfolding. *Nature* **2003**, *426*, 884−890.
(14) Miroy, G. J.; Lai, Z.; Lashuel, H. A.; Peterson, S. A.; Strang, C.; Kelly, J. W. Inhibiting transthyretin amyloid fibril formation via protein stabilization. *Proc. Natl. Acad. Sci. U.S.A.* **1996**, *93*, 15051−15056.
(15) Hammarstrom, P.; Wiseman, R. L.; Powers, E. T.; Kelly, J. W. Prevention of transthyretin amyloid disease by changing protein misfolding energetics. *Science* **2003**, *299*, 713−716.
(16) Johnson, S. M.; Wiseman, R. L.; Sekijima, Y.; Green, N. S.; Adamski-Werner, S. L.; Kelly, J. W. Native state kinetic stabilization as a strategy to ameliorate protein misfolding diseases: A focus on the transthyretin amyloidoses. *Acc. Chem. Res.* **2005**, *38*, 911−921.
(17) Chiti, F.; Taddei, N.; Stefani, M.; Dobson, C. M.; Ramponi, G. Reduction of the amyloidogenicity of a protein by specific binding of ligands to the native conformation. *Protein Sci.* **2001**, *10*, 879−886.
(18) Ray, S. S.; Nowak, R. J.; Brown, R. H., Jr.; Lansbury, P. T., Jr. Small-molecule-mediated stabilization of familial amyotrophic lateral sclerosis-linked superoxide dismutase mutants against unfolding and aggregation. *Proc. Natl. Acad. Sci. U.S.A.* **2005**, *102*, 3639−3644.
(19) Dumoulin, M.; Last, A. M.; Desmyter, A.; Decanniere, K.; Canet, D.; Larsson, G.; Spencer, A.; Archer, D. B.; Sasse, J.; Muyldermans, S.; Wyns, L.; Redfield, C.; Matagne, A.; Robinson, C. V.; Dobson, C. M. A camelid antibody fragment inhibits the formation of amyloid fibrils by human lysozyme. *Nature* **2003**, *424*, 783−788.
(20) Bouchard, M.; Zurdo, J.; Nettleton, E. J.; Dobson, C. M.; Robinson, C. V. Formation of insulin amyloid fibrils followed by FTIR simultaneously with CD and electron microscopy. *Protein Sci.* **2000**, *9*, 960−967.
(21) Bousset, L.; Thomson, N. H.; Radford, S. E.; Melki, R. The yeast prion Ure2p retains its native alpha-helical conformation upon assembly into protein fibrils in vitro. *EMBO J.* **2002**, *21*, 2903−2911.
(22) Souillac, P. O.; Uversky, V. N.; Fink, A. L. Structural transformations of oligomeric intermediates in the fibrillation of the immunoglobulin light chain LEN. *Biochemistry* **2003**, *42*, 8094−8104.
(23) Laurine, E.; Gregoire, C.; Fandrich, M.; Engemann, S.; Marchal, S.; Thion, L.; Mohr, M.; Monsarrat, B.; Michel, B.; Dobson, C. M.; Wanker, E.; Erard, M.; Verdier, J. M. Lithostathine quadruple-helical filaments form proteinase K-resistant deposits in Creutzfeldt-Jakob disease. *J. Biol. Chem.* **2003**, *278*, 51770−51778.
(24) Plakoutsi, G.; Taddei, N.; Stefani, M.; Chiti, F. Aggregation of the Acylphosphatase from *Sulfolobus solfataricus*: The folded and partially unfolded states can both be precursors for amyloid formation. *J. Biol. Chem.* **2004**, *279*, 14111−14119.
(25) Plakoutsi, G.; Bemporad, F.; Calamai, M.; Taddei, N.; Dobson, C. M.; Chiti, F. Evidence for a mechanism of amyloid formation involving molecular reorganisation within nativelike precursor aggregates. *J. Mol. Biol.* **2005**, *351*, 910−922.
(26) Pedersen, J. S.; Christensen, G.; Otzen, D. E. Modulation of S6 fibrillation by unfolding rates and gatekeeper residues. *J. Mol. Biol.* **2004**, *341*, 575−588.
(27) Chow, M. K.; Ellisdon, A. M.; Cabrita, L. D.; Bottomley, S. P. Polyglutamine expansion in Ataxin-3 does not affect protein stability: Implications for misfolding and disease. *J. Biol. Chem.* **2005**, *279*, 47643−47651.
(28) Soldi, G.; Bemporad, F.; Torrassa, S.; Relini, A.; Ramazzotti, M.; Taddei, N.; Chiti, F. Amyloid formation of a protein in the absence of initial unfolding and destabilization of the native state. *Biophys. J.* **2005**, *89*, 4234−4244.
(29) Chiti, F.; Webster, P.; Taddei, N.; Clark, A.; Stefani, M.; Ramponi, G.; Dobson, C. M. Designing conditions for in vitro formation of amyloid protofilaments and fibrils. *Proc. Natl. Acad. Sci. U.S.A.* **1999**, *96*, 3590−3594.
(30) Marcon, G.; Plakoutsi, G.; Canale, C.; Relini, A.; Taddei, N.; Dobson, C. M.; Ramponi, G.; Chiti, F. Amyloid formation from HypF-N under conditions in which the protein is initially in its native state. *J. Mol. Biol.* **2005**, *347*, 323−335.
(31) Zuccotti, S.; Rosano, C.; Ramazzotti, M.; Degl'Innocenti, D.; Stefani, M.; Manao, G.; Bolognesi, M. Three-dimensional structural characterization of a novel Drosophila melanogaster acylphosphatase. *Acta Crystallogr. D Biol. Crystallogr.* **2004**, *60*, 1177−1179.
(32) Corazza, A.; Rosano, C.; Pagano, K.; Alverdi, V.; Esposito, G.; Capanni, C.; Bemporad, F.; Plakoutsi, G.; Stefani, M.; Chiti, F.; Zuccotti, S.; Bolognesi, M.; Viglino, P. Structure, conformational stability, and enzymatic properties of acylphosphatase from the hyperthermophile *Sulfolobus solfataricus*. *Proteins* **2006**, *62*, 64−79.
(33) Degl'Innocenti, D.; Ramazzotti, M.; Marzocchini, R.; Chiti, F.; Raugei, G.; Ramponi, G. Characterization of a novel *Drosophila melanogaster* acylphosphatase. *FEBS Lett.* **2003**, *535*, 171−174.
(34) Taddei, N.; Stefani, M.; Vecchi, M.; Modesti, A.; Raugei, G.; Bucciantini, M.; Magherini, F.; Ramponi, G. Arginine-23 is involved in the catalytic site of muscle acylphosphatase. *Biochim. Biophys. Acta* **1994**, *1208*, 75−80.
(35) Taddei, N.; Stefani, M.; Magherini, F.; Chiti, F.; Modesti, A.; Raugei, G.; Ramponi, G. Looking for residues involved in the muscle acylphosphatase catalytic mechanism and structural stabilization: Role of Asn41, Thr42, and Thr46. *Biochemistry*. **1996**, *35*, 7077−7083.
(36) Taddei, N.; Chiti, F.; Magherini, F.; Stefani, M.; Thunnissen, M. M.; Nordlund, P.; Ramponi, G. Structural and kinetic investigations on the 15−21 and 42−45 loops of muscle acylphosphatase: Evidence for their involvement in enzyme catalysis and conformational stabilization. *Biochemistry* **1997**, *36*, 7217−7224.
(37) Stefani, M.; Taddei, N.; Ramponi, G. Insights into acylphosphatase structure and catalytic mechanism. *Cell. Mol. Life Sci.* **1997**, *53*, 141−151.
(38) Santoro, M. M.; Bolen, D. W. Unfolding free energy changes determined by the linear extrapolation method. 1. Unfolding of phenyl-methanesulfonyl alpha-chymotrypsin using different denaturants. *Biochemistry* **1988**, *27*, 8063−8068.
(39) Bemporad, F.; Capanni, C.; Calamai, M.; Tutino, M. L.; Stefani, M.; Chiti, F. Studying the folding process of the acylphosphatase from *Sulfolobus solfataricus*. A comparative analysis with other proteins from the same superfamily. *Biochemistry* **2004**, *43*, 9116−9126.
(40) Plakoutsi, G.; Bemporad, F.; Monti,M.; Pagnozzi, D.; Pucci, P.; Chiti, F. Exploring the mechanism of formation of native-like and precursor

amyloid oligomers for the native acylphosphatase from *Sulfolobus solfataricus*. *Structure* **2006**, *14*, 993−1001.
(41) Camici, G.; Manao, G.; Cappugi, G.; Ramponi, G. A new synthesis of benzoyl phosphate: A substrate for acyl phosphatase assay. *Experientia* **1976**, *32*, 535−536.
(42) Ramponi, G.; Treves, C.; Guerritore, A. A. Aromatic acyl phosphates as substrates of acylphosphatase. *Arch. Biochem. Biophys.* **1966**, *115*, 129−135.
(43) Johnson, W. C., Jr. Protein secondary structure and circular dichroism: A practical guide. *Proteins* **1990**, *7*, 205−214.

JM0606488